08/25/99

The role of self-organized criticality in the substorm phenomenon and its relation to localized reconnection in the magnetospheric plasma sheet

A. J. Klimas

NASA / Goddard Space Flight Center, Greenbelt, Maryland

J. A. Valdivia

Universities Space Research Association, Seabrook, Maryland

D. Vassiliadis

Universities Space Research Association, Seabrook, Maryland

D. N. Baker

Laboratory for Atmospheric and Space Physics, University of Colorado, Boulder, Colorado

M. Hesse

NASA / Goddard Space Flight Center, Greenbelt, Maryland

J. Takalo

Visiting Scientist, NASA / Goddard Space Flight Center, Greenbelt, Maryland

Abstract. Evidence is presented that suggests there is a significant self-organized criticality (SOC) component in the dynamics of substorms in the magnetosphere. Observations of BBFs, fast flows, localized dipolarizations, plasma turbulence, etc. are taken to show that multiple localized reconnection sites provide the basic avalanche phenomenon in the establishment of SOC in the plasma sheet. First results are presented from a continuing plasma physical study of this avalanche process. A one-dimensional resistive MHD model of a magnetic field reversal is discussed. Resistivity, in this model, is self-consistently generated in response to the excitation of an idealized current-driven instability. When forced by convection of magnetic flux into the field reversal region, the model yields rapid magnetic field annihilation through a dynamic behavior that is shown to exhibit many of the characteristics of SOC. Over a large range of forcing strengths, the annihilation rate is shown to self-adjust to

balance the rate at which flux is convected into the reversal region. Several analogies to magnetotail dynamics are discussed: (1) It is shown that the presence of a localized criticality in the model produces a remarkable stability in the global configuration of the field reversal while simultaneously exciting extraordinarily dynamic internal evolution. (2) Under steady forcing, it is shown that a loading-unloading cycle may arise that, as a consequence of the global stability, is quasi-periodic and, therefore, predictable despite the presence of internal turbulence in the field distribution. Indeed, it is shown that the global loading-unloading cycle is a consequence of the internal turbulence. (3) It is shown that, under steady, strong forcing the loading-unloading cycle vanishes. Instead, a recovery from a single unloading persists indefinitely. The field reversal is globally very steady while internally it is very dynamic as field annihilation goes on at the rate necessary to match the strong forcing. From this result we speculate that steady magnetospheric convection events result when the plasma sheet has been driven close to criticality over an extended spatial domain. During these events, we would expect to find localized reconnection sites distributed over the spatial domain of near criticality and we would expect to find plasma sheet transport in that domain to be closely related to that of BBF and fast flow events.

I. Introduction

The magnetospheric substorm is a coherent global phenomenon that evolves predictably through a sequence of clearly recognizable phases [*Baker et al.*, 1996; 1999]. Recent Geotail spacecraft observations generally support the near-Earth neutral line (NENL) model of this evolution. In particular, the plasma sheet region 20-30 R_E tailward of Earth has been identified as the most probable location of the NENL early in the substorm expansion phase and the commencement of reconnection at the NENL has been associated with the substorm onset [*Nagai et al.*, 1998].

Within the NENL model, loading of magnetic flux into the magnetotail leads to a substorm growth phase during which the plasma and current sheet are stretched tailward and thinned [*Pulkkinen et al.*, 1992; 1994a; 1994b; 1998]. The substorm is predominantly a mechanism for unloading this excess magnetic energy and relieving the stressed plasma sheet [*Baker et al.*, 1997]. The onset of reconnection at the NENL is not well understood, but it is clear that a critical state must be reached for this onset to occur; magnetic flux loading typically proceeds for 50-60 min before this critical state can be reached [*Baker et al.*, 1986].

Recent observations of the magnetotail plasma sheet have shown it to be a dynamic and turbulent region. *Borovsky et al.* [1997] have found strong turbulence in the plasma sheet at $= 20\ R_E$ tailward of Earth, close to the average position of the NENL; the turbulence is observed at all geomagnetic activity levels. These turbulent magnetic and velocity fields are most certainly related to the high-speed, bursty bulk flows of the inner central plasma sheet [*Baumjohann et al.*, 1990; *Angelopoulos et al.*, 1992; 1994; 1996]. Detailed studies of the Geotail plasma sheet data have revealed high-speed flow bursts, plasma vortices, and corresponding strongly varying magnetic field [*Fairfield et al.*, 1998; 1999; *Lyons et al.*, 1999]. In the distant tail ($= 200\ R_E$) the turbulent magnetic field forms power-law power spectra [*Hoshino et al.*, 1994]. Closer to Earth, ($< 10\ R_E$) *Ohtani et al.* [1995; 1998] have described AMPTE/CCE and SCATHA observations of magnetic fluctuations associated with substorm onset as due to a system of turbulent and chaotic filamentary electric currents. *Nagai et al.* [1998] found that magnetic reconnection in the vicinity of the NENL lasts for approximately 10 min, stopping even while the substorm expansion phase proceeds, implying that reconnection occurs at localized sites that either move rapidly or turn on and off over the course of a substorm.

The appearance of strong turbulence in the plasma sheet, in particular in the region associated with substorm onset, may seem incompatible with the coherence and repeatability of the substorm cycle. It is difficult to understand the existence of a critical state and the sudden transition from global stability to instability in plasma that is strongly turbulent even before the transition. It appears that localized, intermittent reconnection plays a role in this transition. But the mechanism by which these localized, intermittent reconnection sites are organized into the global coherent magnetospheric substorm remains unexplored [*Baker et al.*, 1999].

Below, we review a variety of evidence that strongly suggests the magnetotail is driven through flux transfer from the dayside magnetopause into a state of "self-organized criticality" (SOC). It is an important property of physical systems that evolve into SOC that they self-organize toward a unique global state. In this state, internal small-spatiotemporal-scale system phenomena are unpredictable and can only be described statistically. Nevertheless, this critical global state is inevitable, and repeatable. This is the basis, we propose, for the global coherence and repeatability of the substorm phenomenon in the turbulent plasma sheet. At or near substorm onset, the plasma sheet can be described as being in a global SOC state containing significant small-scale turbulence. A quantitative characterization of that global SOC state is a primary goal of our research. In this paper we report the first results from this research.

We study the magnetospheric substorm phenomenon as an avalanche of many small reconnection events in the turbulent plasma sheet under the assumption that it is in, or near, a SOC state. In the SOC state, such avalanches

occur over a broad distribution of spatial and temporal scales, ranging from localized events, which we associate with flow bursts, to "system wide" events, substorms, in which a significant portion of the plasma sheet is lost in the form of plasmoids. Our approach is guided by several recent studies in which "sandpile" models [*Consolini*, 1997; *Chapman et al.*, 1998; *Uritsky and Pudovkin*, 1998] and "coupled-map lattice" models [*Takalo et al.*, 1999a; 1999b] (both discussed below) were driven into SOC and then shown to thereby reproduce various measures of substorm activity. Based on the available evidence for SOC in the plasma sheet, combined with the successes of these early sandpile and coupled-map lattice model studies, we have begun an investigation of plasma physical models of the plasma sheet that appear to evolve into SOC. Our goal is to understand the conditions under which the plasma sheet may evolve into SOC and, further, to understand the role of this plasma sheet in the substorm phenomenon.

In the following section we present primarily observational evidence in support of our contention that the plasma sheet is in SOC, or something very similar to it. Then, in section III we give a brief review of some basic properties of systems in SOC and we discuss the relationship between discrete and continuum models of SOC. In section IV we introduce a resistive MHD model of a magnetic field reversal, relate it to a general model introduced earlier by *Lu* [1995a], and present a detailed analysis of the model behavior. Our principal result is a magnetic field reversal model in which fast field annihilation is achieved through a dynamic process that exhibits many of the properties of a system in SOC. Section V contains a summary of our results. Although the field reversal model is a highly idealized representation of the plasma sheet, we are able, nevertheless, to make several conjectures on the magnetotail substorm dynamics based on our results.

II. Evidence for the Self-Organized Critical Plasma Sheet

Self-organized criticality is a state to which dissipative systems evolve naturally under loading of a conserved quantity, being unable to unload until reaching a critical state in which a localized threshold instability is excited which allows rapid transport of the conserved quantity out of the system. It is now well established that loading of magnetic flux into the magnetotail during the substorm growth phase leads to thinning of the plasma sheet and intensification of the current sheet to the point of instability, and thus unloading [*Baker et al.*, 1996].

Although there is no experimental proof that the magnetotail is in a SOC state, there are several pieces of evidence that support the conjecture quite effectively.

Extended power-law distributions in auroral geomagnetic disturbances

An important feature of many systems that exhibit SOC is that they dissipate their stored energy in "avalanches" characterized by power-law distributions for avalanche size and duration. In addition, power-law power spectra are found associated with the internal energy dissipation and system output time series. Assuming that the *AE* index is an indirect measure of energy dissipation, *Consolini* [1997] has examined 1 year (1978) of 1 min resolution *AE* index data for these effects. To measure avalanche size, Consolini defined a "burst strength"

$$s = \int_{\Omega} \left(AE(t) - L_{AE} \right) dt \tag{1}$$

in which L_{AE} is a fixed measure of quiet conditions in the *AE* index and Ω is the time interval over which the condition $AE(t) \geq L_{AE}$ is satisfied. Nearly 3000 events were defined in this manner and a distribution of bursts strengths $D(s)$ was constructed. Consolini found that $D(s) \propto s^{-1}$ over more than 4 decades in burst strength. Consolini also constructed a power spectrum for these *AE* index data. The spectrum consists of two power-law spectral regions, the low frequency portion with slope $\simeq$ -1 and the high frequency portion with slope $\simeq$ -1.9, separated by a break at the frequency $f_A = 1/4.3$ hrs^{-1}, in agreement with results that had been obtained earlier by *Tsurutani et al.* [1990]. In addition, Consolini was able to use the running sandpile model of *Hwa and Kardar* [1992] to reproduce this power spectrum.

With the assumption that the solar wind input to the magnetosphere can be approximated by stochastic noise, the results of Consolini are strong evidence that the *AE* index data are the result of a self-organized critical phenomenon in the magnetosphere. We assume that this phenomenon occurs in the plasma sheet.

Bursty bulk flow events

We hypothesize local reconnection sites that are much smaller than the dimensions of the plasma sheet and that provide the basic avalanche phenomenon in the establishment of SOC in the plasma sheet. Bursty bulk flow (BBF) events containing high-speed flows have been observed in the inner central plasma sheet [*Baumjohann et al.*, 1990; *Angelopoulos et al.*, 1992]; these may be related to localized reconnection sites. Angelopoulos et al. have shown that BBFs are short lived events, lasting approximately 10 min and containing very large amplitude velocity peaks lasting characteristically 1 min, with both temporal and spatial effects responsible for their bursty nature. These events are usually associated with magnetic field dipolarizations and ion temperature increases and they are responsible for most of the earthward transport of magnetic field, plasma density and energy. In a statistical study of bursty bulk flow events, *Angelopoulos et al.* [1994] have found that they correlate with the *AE* index, and they have suggested that BBFs are associated with geomagnetic activity. In a detailed study of a single BBF, *Angelopoulos et al.* [1996] put an upper bound on the spatial extent of the flow in the Y-Z directions at 1-2 R_E. Further, they concluded, on the

basis of the flux content convected past the AMPTE/IRM spacecraft, that lobe flux reconnection must have occurred tailward of the spacecraft in this event. On the basis of these observations, Sergeev et al. [1996b] have postulated impulsive dissipation events, localized in space and time, which are the manifestations of tail reconnection. They suggested two competitive processes responsible for energy storage and dissipation during substorm and non-substorm times; a slow reconfiguration associated with energy storage and a sequence of local, sporadic, short-term energy dissipation events. More recently, *Fairfield et al.* [1998] studied a single event observed on Geotail in the near-equatorial magnetotail at 13 R_E and 2300 LT and associated with a substorm onset. Fairfield et al. reported intense earthward flow at 2000 km/s perpendicular to the northward magnetic field and lasting approximately 1 minute. Subsequent to the onset, they noted plasma vortices punctuated by occasional flow bursts and violently varying magnetic field. Fairfield et al. concluded the rapid flow had a small cross-tail dimension of the order of 1 R_E and was associated with reconnection tailward of the spacecraft. In a continuation of this work, *Fairfield et al.* [1999] demonstrated the association of isolated $\approx$ 1 min fast flows (up to 1000 km/sec) with auroral brightening, AKR onsets, geosynchronous particle injections, and ground magnetic activity. Fairfield et al. concluded that these phenomena were initiated in the tail beyond 15 R_E, presumably by magnetic reconnection. But the particular events studied by *Fairfield et al.* [1999] were not associated with auroral expansion. *Nagai et al.* [1998], in a study of many substorm onsets with Geotail observations, found that magnetic reconnection is localized to the premidnight sector of the magnetotail at 20-30 R_E. Further, they found that, at the position of the spacecraft, magnetic reconnection lasts for approximately 10 min, stopping even while the substorm expansion phase proceeds, and thus implying that reconnection occurs at localized sites that either move rapidly or turn on and off over the course of a substorm.

All of the above observations are consistent with our assumption of multiple localized reconnection sites as the basic avalanche phenomenon in the establishment of SOC in the plasma sheet.

Self-similar current and magnetic field topologies in the distant plasma sheet

Physical systems that evolve into self-organized criticality are spatially extended and dynamic; they evolve both temporally and spatially. When in the SOC state these systems exhibit no characteristic time or length scale over a broad range of such scales. These systems exhibit self-similar spatial structure; i.e., fractal topology. These appear to be characteristics of the plasma sheet.

Hoshino et al. [1994] have discussed Geotail magnetic field observations in the distant plasma sheet ($\approx$ 200 R_E) in terms of a turbulent magnetic reconnection process. They showed that most of the data are characterized by "kink" power-law power spectra containing two spectral indices separated by a critical frequency.

M *et al.* [1996] have provided an explanation for the magnetic field observations of *Hoshino et al.* [1994] in ter self-consistent model of the magnetic field structures in the distant plasma sheet. Their model predicts fract etic structures in the range of spatial scales between $\approx 4\times10^2$ km and $\approx 8\times10^3$ km. Milovanov et al. expl e position of the kink frequency in the Hoshino et al. spectra and predicted the position of a second, high ency, kink. In addition, they explained the values of the spectral indices on either side of the observed kink model is of an ensemble of magnetic field flux tubes with a self-similar spatial distribution in the range of s cales given above. They argued that "... the existence of the two kinks could be a result of self-orga n of currents and magnetic fields in the distant tail related to the development of fractal topologies in the rang patial scales between 4×10^2 km and 8×10^3 km."

Th ulent plasma sheet nearer Earth

ky et al. [1997] have studied the bulk flow and magnetic field fluctuations during 10 several-hour long int when the ISEE-2 spacecraft was in the plasma sheet at $\approx$ 20 R_E behind Earth. Their results show a strongly tu t plasma sheet with fluctuations in the flow velocity much larger than the mean flow and fluctuations in the ma ic field comparable to average values. They found that this description of the plasma sheet applies during any ph f geomagnetic activity, even including steady magnetospheric convection intervals. They constructed power sp for the bulk flow and magnetic field fluctuations that, although limited in spectral range, showed power-law fre ncy dependence. The results of Borovsky et al. are in sharp contrast to a picture of plasma sheet transport in w drifts lead to laminar earthward flow in a well ordered magnetic field.

ani et al. [1995; 1998] have studied magnetic field fluctuations in the near-Earth tail at substorm onset times us data from the AMPTE/CCE and SCATHA (1998 study only) spacecraft. In their earlier study, they found po r-law power spectra for these fluctuations but their emphasis has been on a time-series fractal dimension analy-sis n both studies Ohtani et al. found that the magnetic field fluctuations are due to a system of perturbation electric cu nts in the tail current sheet associated with tail current disruption at substorm onset; they describe these as tur-bu t and chaotic filamentary electric currents.

he results discussed in this section, as well as some of the results discussed above [*Baumjohann et al.*, 1990; *A elopoulos et al.*, 1992; 1994; 1996; *Fairfield et al.*, 1998; 1999], indicate strong turbulence in the plasma sheet ne er Earth. We are unaware of an analysis such as that done by *Milovanov et al.* [1996] on the *Hoshino et al.* [1 94] Geotail observations, but using data from nearer earth regions. Thus we cannot argue as strongly that these ob ervations indicate SOC in this region, but we do emphasize that these observations are consistent with SOC.

Pi2 pulsations

These magnetic pulsations are signatures of plasma sheet turbulence and self-organization before the release of excess energy. As the plasma sheet is compressed during the late growth phase of substorms, a series of Pi2 pulsations, separated by 5-10 min, appears shortly before the onset and are considered one of its indicators [*Saito et al.*, 1976; *Sakurai and Saito*, 1976]. *McPherron and Hsu* [1998] have compared the timing information from each Pi2 peak to other indicators (auroral precipitation, poleward retraction of the oval, high-latitude magnetograms) and have found that the early peaks precede the substorm indicators, while the last one (which they call the "main onset") coincides with the other signatures. Their interpretation is that the pulsations correspond to local plasma sheet regions becoming temporarily unstable, but their effect is quenched before it can affect global stability. Hence the growth phase does not evolve monotonically towards onset, but goes through several metastable or even locally unstable states. This is strikingly similar to the conditions for a system to develop self-organized criticality [*Lu*, 1995a].

Low-dimensional magnetospheric dynamics

The magnetosphere behaves as a low-dimensional dynamical system in many respects [*Klimas et al.*, 1996]. Modern input-output methods, which either rely on the system being low dimensional, or show that it is low dimensional, have been quite successful in modeling and/or predicting the geomagnetic activity of the magnetosphere. Perhaps the most important results, in this respect, were obtained by *Vassiliadis et al.* [1995] who, using empirical nonlinear filters and upstream solar wind data for input, were able to effectively predict electrojet index data and simultaneously show that the dynamics of the empirical filters are low dimensional. The methods used by Vassiliadis et al. have also been used to predict *Dst* index data [*Valdivia et al.*, 1996], and more recently have been applied successfully to predict the spatial distribution of magnetic disturbances on Earth's surface [*Valdivia et al.*, 1999a; 1999b]. Moreover, low-dimensional physics based models [*Klimas et al.*, 1992; 1994; *Horton and Doxas*, 1996; *Horton et al.*, 1998; *Horton and Doxas*, 1998] have been shown to replicate many of the features of the solar wind-magnetosphere interaction over very long intervals of electrojet index data. Recently, empirical analogues have been constructed [*Klimas et al.*, 1997; 1998; 1999] that combine the methods used by Vassiliadis et al. with the physics based methods. These are data-derived low-dimensional models that have been shown to both model the magnetospheric dynamics and predict the *Dst* and electrojet index responses.

The plasma sheet is a key component in the dynamics of the magnetosphere, particularly with respect to the substorm dynamics. We have shown above that the plasma sheet is strongly turbulent. It is difficult to understand how a dynamical system containing a strongly turbulent key component can exhibit apparently low dimensional behavior.

But *Chang* [1992a; 1992b; 1998] has shown that this is exactly the behavior to be expected from a system in SOC and studies of turbulent transport in magnetically confined plasmas have confirmed this [*Diamond and Hahm*, 1995; *Newman et al.*, 1996; *Carreras et al.*, 1996].

Summary

We believe that the evidence overwhelmingly supports the presence of a SOC component in the central plasma sheet that is instrumental in the development of the substorm cycle. Although the SOC paradigm is a new and unfamiliar one, it does not appear possible to proceed further in understanding the substorm process without examining the implications of SOC in the process.

III. Discrete and Continuum Models of Self-Organized Criticality

Physical systems that are open (subject to throughput; loading, transport, unloading), dissipative, spatially distributed, and driven by an external loading process often evolve to a critical state far from equilibrium that has been called self-organized criticality [*Bak et al.*, 1987; 1988]. In such a state the temporal output of the system is intermittent and characterized by power-law power spectra while its spatial structure exhibits scale-invariant, self-similar (fractal) properties.

It is remarkable that the SOC state is a robust state (it does not depend on the details of the dynamics and the physics of the system); it occurs in a variety of plasma and fluid environments [*Lu and Hamilton*, 1991; 1993; 1995b; 1995c; *Vlahos et al.*, 1995; *Diamond and Hahm*, 1995; *Newman et al.*, 1996; *Carreras et al.*, 1996; 1998]. The statistical behavior of many complex distributed systems appears to be more a property of their self-organized critical state, if it is achieved, than the details of the physical processes that allow the critical state. In the plasma sheet, for example, it is possible that the statistics of substorms, pseudobreakups, and even the evolutions of the growth and expansion phases, are unrelated to the details of the reconnection process other than that reconnection allows for the establishment of a SOC state.

Following the seminal study of *Bak et al.* [1987], a variety of sandpile models have been shown to evolve naturally into a SOC state (in particular, see the "running" sandpile model of *Hwa and Kardar* [1992]).

Sandpile models

Sandpile models [*Bak et al.*, 1987; 1988; *Hwa and Kardar*, 1992; *Consolini*, 1997; *Chapman et al.*, 1998; *Uritsky and Pudovkin*, 1998] are cellular automata in which discrete "grains" of a conserved quantity are added to an array of cells and then moved from one cell to the next according to a set of rules. Coupled-map lattice models [*Takalo et*

al., 1999a; 1999b] are similar to the sandpile models, except that the conserved quantity is transported in a continuum of grain sizes. Generally the grains do not move until a critical condition is exceeded in one of the cells, at which point a portion of the grains in that cell is distributed into the surrounding cells. Following this distribution it may be that one of the receiving cells has been driven above the critical condition and thus a further distribution follows. In this way an avalanche may result in which many cells take part in the response to the introduction of a single grain in one of the cells. When the grains reach an open boundary they are removed from the system. Under certain conditions such a system can reach a quasi-steady state in which the long-term average rate at which grains leave the system is equal to the long-term average rate at which they are introduced while avalanches of all sizes take part in the transport of grains to the open boundary. For reference, a true sandpile can be imagined on which the slope of the sandpile is almost unstable everywhere. It should be noted, however, that we have found the evolution of the plasma physical model that we discuss below to be considerably more dynamic than that suggested by this image. An important feature of the sandpile models is that they are extremely fast computational tools for examining the evolution of physical systems that are in SOC.

The sandpile and coupled-map lattice models, however, are rather abstract models of the physical systems that they represent. These models are inherently discontinuous; they are iterated on a discrete grid with time evolving in a series of discontinuous steps. Further, a field quantity that usually represents a conserved quantity is transported from grid point to grid point according to a set of simple rules. Such models seem so far from the continuous physical world that we might ignore them were it not for the fact that they are effective in representing many facets of the substorm phenomenon [*Consolini*, 1997; *Chapman et al.*, 1998; *Uritsky and Pudovkin*, 1998; *Takalo et al.*, 1999a; 1999b] while incorporating the SOC dynamics that does appear to be an important feature of the central plasma sheet. Fortunately, several studies have been carried out to discover under what conditions more realistic continuum models of physical systems (for example, hydrodynamic or MHD systems), as opposed to cellular automata, may evolve into SOC.

Criteria for SOC in continuum physical systems

In the culmination of a sequence of papers [*Lu and Hamilton*, 1991; *Lu et al.*, 1993] concerning the spatiotemporal distribution of solar flares, *Lu* [1995a] has given a list of criteria that a physical system (not an automaton model) must satisfy in order to exhibit SOC behavior. The following is a quote from Lu (enumeration added):

"To summarize, we expect that driven dissipative systems which meet the following criteria can be naturally driven to a state with a broad power-law distribution of discrete energy dissipating events. (1) First, there must be a locally conserved field which is subject to a threshold instability. (2) The instability leads to rapid local diffusion of the

field, which dissipates energy and locally stabilizes the field. (3) The field must have metastable states in which energy can be built up by the driving term. (4) The slow evolutionary time scale of these metastable states must be very much slower than the rapid instability time scale, and (5) the driving time scale must be intermediate between the two. Furthermore, (6) any intrinsic length scales associated with the instability must be very much less than the size of the system. Finally, (7) the system must be driven for a long enough period for it to settle to a steady state."

It is remarkable that, although developed in the context of an unrelated discussion, each of these criteria are satisfied by our present understanding of the magnetotail dynamics involved in the substorm cycle: (1) The conserved field is magnetic flux (as calculated, e.g. by considering the intersection of field lines with the equatorial plane); it is subject to a threshold instability that is not fully understood at present, but which is known to lead to reconnection which reconfigures the flux lines and conserves them. (2) In the reconnection process, flux lines are rapidly transported into and out of a reconnection site with the consequent dissipation of lobe field energy. That this process stabilizes the field can only be inferred from the fact that every observed bursty bulk flow event does not lead to a substorm, which would be the case if stabilization did not occur. (3) The metastable states correspond to the magnetotail state during the growth phase. (4) Translated into substorm physics, the time scale under discussion in this point is a measure of the interval necessary for the magnetotail to relax back to a "ground state," having been loaded by flux transfer from the dayside. This is a measure of the time necessary to reconnect the excess open lobe flux at the "distant neutral line" and convect it back to the dayside magnetosphere. Estimates are several hours or more, certainly much longer than the growth time of the localized instability that leads to reconnection nearer Earth. (5) The substorm growth phase typically lasts for 1 hour, or somewhat less, which is indeed between the instability growth time and the metastable state relaxation time. (6) The localized reconnection sites that we consider are much smaller than the dimensions of the plasma sheet. We discuss some of the available evidence in support of this picture in the next section. (7) The meaning of a steady state in this context must be understood. A system in SOC never reaches a truly steady state. What is meant is that, when averaged over a time scale that is large compared to the interval between avalanches of any size, and large compared to any fluctuation time scales in the driver, the system has a steady state. This steady state is reached if equilibrium between input and output can be achieved over sufficiently long time scales. We assume that the magnetotail has an average flux content which is neither growing nor decaying when averaged over an interval that is long compared to all time scales associated with substorm dynamics and/or solar wind variability.

The necessary conditions given above in the quote by *Lu* [1995a] must be satisfied for a continuum system to evolve into SOC. As we have shown above, Lu's criteria are satisfied in the magnetotail. *Lu* [1995a] also introduced a nonlinear diffusion model that satisfies his criteria and showed that it evolves into SOC. We will discuss a variant

of this model thoroughly below and show that it is the core element of a resistive MHD model of the central plasma sheet in which the effective resistivity varies rapidly in space and time.

IV. Self-Organized Criticality in a Continuum Model

We have presented Lu's criteria [*Lu*, 1995a] that a physical system must satisfy in order to exhibit SOC behavior, and we have shown that these criteria are satisfied by the magnetotail dynamics involved in the substorm cycle. Lu also discussed a continuum model that satisfies his criteria and evolves into SOC. In this section we give a brief review of Lu's continuum model, and show that it is the element of a resistive MHD model of the plasma sheet current layer that allows for localized reconnection. Thus the Lu continuum model provides a link between the sandpile model studies mentioned above and a realistic plasma physical study of SOC dynamics in the plasma sheet. We examine the behavior of the model in detail as it relates to plasma sheet dynamics.

The Lu model

The continuum model of *Lu* [1995a] is given by

$$\frac{\partial \varphi(z,t)}{\partial t} = \frac{\partial}{\partial z}\left[D(z,t)\frac{\partial \varphi}{\partial z}\right] + S(z,t) \tag{2}$$

$$\frac{\partial D(z,t)}{\partial t} = \frac{Q\left(\left|\partial \varphi / \partial z\right|\right)}{\tau} - \frac{D}{\tau} \tag{3}$$

$$Q\left(\left|\partial \varphi / \partial z\right|\right) = \begin{cases} D_{\min} & \text{low state, } \left|\partial \varphi / \partial z\right| < k \\ D_{\max} & \text{high state, } \left|\partial \varphi / \partial z\right| > \beta k \end{cases} \tag{4}$$

in which $\varphi(z,t)$ is a scalar field, $D(z,t)$ is a variable diffusion coefficient, $S(z,t)$ is a source term, and $D_{\max} >> D_{\min}$. The quantity $Q(z,t)$ is double valued and depends on the history of $\left|\partial \varphi / \partial z\right|$, k represents an instability threshold, and $0 < \beta < 1$. It is important to realize that $Q(z,t)$ varies both spatially and temporally. At a given position, Q remains in the low state, $Q = D_{\min}$, until the slope satisfies $\left|\partial \varphi / \partial z\right| > k$, whereupon it undergoes a transition to the high state. However, when in the high state Q does not make the transition to the low state until the slope $\left|\partial \varphi / \partial z\right| < \beta k$. Thus Q acts like a physical instability in that the value of the slope k required to turn on the instability is greater than the value βk required to maintain the instability once it is turned on.

The diffusion coefficient $D(z,t)$ evolves in response to Q. When Q switches to $D_{\max}$, the diffusion coefficient $D(z,t)$ begins to rise toward $D_{\max}$. If the absolute value of the local slope remains above k for a time longer than of order τ, then the diffusion coefficient saturates at $D = D_{\max}$. Once the instability is turned off, the diffusion coeffi-

cient decays back to D_{min} with time constant τ. At any position z the evolution of both $Q(z,t)$ and $D(z,t)$ is independent of either of these quantities at any other position. Completely disordered evolution is possible; ordered evolution that may develop is self-organized.

Resistive MHD Field Reversal Model

Lu [1995a] studied solutions of the system (2)-(4) that mimic those of sand pile models. Through the source $S(z,t)$, field $\varphi(z,t)$ was added to a "pile" and the dynamics of the system developed as the slope of the pile increased and consequently the field migrated to open boundaries where it was removed. With a different source function, and modified boundary conditions, the Lu model, system (2)-(4), becomes a 1-dimensional resistive MHD model of a magnetic field reversal in which the dynamics of the system are due to spatiotemporal magnetic field annihilation. This simplified current sheet model is developed and studied below. We present this model as the first step in the development of a resistive MHD plasma sheet model in which kinetic effects that lead to localized reconnection at small spatial scales are modeled as time-dependent and spatially localized anomalous resistivity.

We start with the resistive MHD assumption

$$\nabla \times \boldsymbol{E} + \frac{1}{c}\frac{\partial \boldsymbol{B}}{\partial t} = 0 \tag{5}$$

$$\nabla \times \boldsymbol{B} = \frac{4\pi}{c}\boldsymbol{J} \tag{6}$$

$$\boldsymbol{J} = \frac{1}{\eta}\left(\boldsymbol{E} + \frac{\boldsymbol{V}}{c} \times \boldsymbol{B}\right) \tag{7}$$

in which η is a spatiotemporal resistivity. Assuming that all quantities depend on only a single spatial variable z and that the magnetic field has only an x-component, then

$$\frac{\partial B_x}{\partial t} = \frac{\partial}{\partial z}\left[D(z,t)\frac{\partial B_x}{\partial z}\right] + S(z,t) \tag{8}$$

in which

$$S(z,t) = -\frac{\partial}{\partial z}(V_z B_x) \tag{9}$$

with the diffusion coefficient $D(z,t) = (c^2/4\pi)\eta(z,t)$ and the current $J_y = (c/4\pi)\partial B_x/\partial z$. Comparing (8) to (2), we see that the Lu model can be viewed as a 1-dimensional resistive MHD model in which the resistivity is gener-

ated self consistently. From this viewpoint, the diffusion is due to anomalous resistivity that waxes and wanes in response to the excitation and quenching of a current driven instability; one that is excited when the current density gets above a critical level [*Papadopoulos*, 1985; *Lui et al.*, 1991; 1993; 1995; *Yoon and Lui*, 1996] and is quenched when the current density is driven below a level that is lower than the critical one.

We study solutions of (8) on a spatial interval $-L \le z \le L$ subject to boundary conditions $\partial B_x / \partial z = 0$ at $z = \pm L$. Thus, in contrast to the *Lu* [1995a] solutions, there is no transport of B_x through the boundaries in these solutions. We restrict our solutions to those that are antisymmetric in z; our solutions contain a field reversal at $z = 0$. In addition, we assume that V_z also reverses sign at $z = 0$ in the sense that (9) represents convection of B_x into the field reversal region from outside; we treat $S(z,t)$ as a given source function and thus decouple (8) from the rest of the MHD system. Specifically, we choose $S(z,t) = S(z) = S_0 \sin(\pi z / 2L)$. This source function has the effect of steadily increasing the strength of the field reversal and steadily increasing the strength of the current sheet that supports

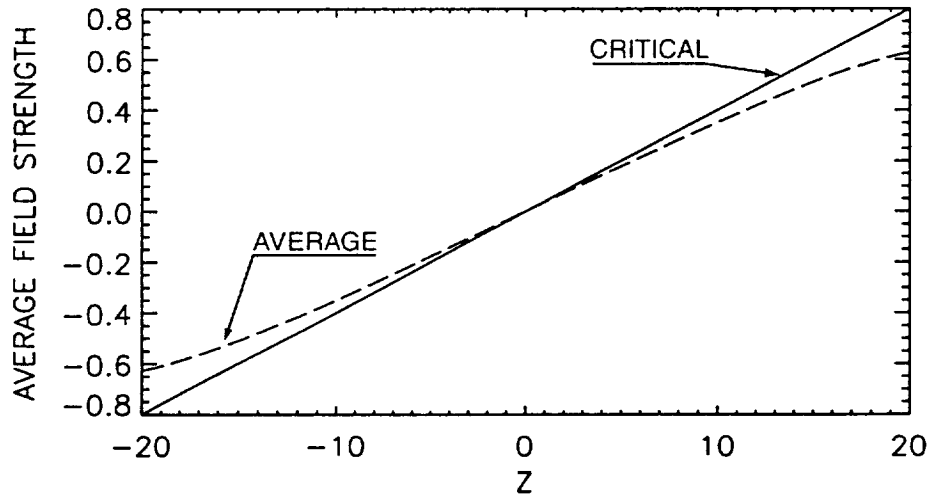

Figure 1. Slope of time averaged field strength lies below critical slope at all positions.

the field reversal. The choice of an initial condition for B_x appears arbitrary; eventually the system evolves into a dynamic state in which the increasing strength of the field reversal that is induced by the source function is balanced, on average, by magnetic field annihilation in the current sheet. We demonstrate below, for a certain range of model parameters, that when this state is reached the model exhibits many of the properties of a system in SOC.

Analysis

We integrate the system (2)-(4), with $\varphi(z,t)$ replaced by $B_x(z,t)$, using a source $S(z)$ that is constant in time as discussed above. Initially, we set $Q(z,0) = D_{min}$ and $D(z,0) = D_{min}$. It appears that the choice for $B_x(z,0)$ is arbitrary. For a set of test integrations, we have found that the system evolves through a transient into a dynamical behavior that is independent of the initial state. Generally, to achieve this behavior as quickly as possible, we initialize B_x so that its gradient is just above the critical gradient k over a significant portion of the spatial interval $[-L, L]$. For all of the results discussed below, we have set $\partial B_x / \partial z = 0$ at the boundaries of the discrete spatial grid on which we integrate the system.

In response to the source $S(z,t) = S(z) = S_0 \sin(\pi z / 2L)$, the field $B_x(z,t)$ evolves into a reversed field configuration. Eventually, criticality is reached at some position, leading to a remarkably complex sequence of avalanche-like events that carry flux through the system. The result is a time-averaged state, an example of which is shown in Figure 1, whose slope lies close to, but below, the critical gradient. This difference between average state and critical state is central to the evolution of the system; it will be discussed further below.

We have examined the behavior of (2)-(4) over a wide range of the parameters S_0 (the source strength) and D_{min} while holding the remaining model parameters fixed at the values chosen by Lu; $\tau = 1$ (the fundamental time-scale in the model), $D_{max} = 5$, $k = 0.04$, and $\beta = 0.9$. In addition, we have studied some of the effects of varying the parameter β. For large D_{min} ($\approx$ 0.1 and greater) the system settles into a simple periodic evolution. For smaller D_{min}, an irregular loading-unloading cycle arises over a range of S_0 values that varies with D_{min}. The amplitude of the loading-unloading cycle depends primarily on D_{min}, not S_0; it decreases as D_{min} decreases. In the following we discuss the behavior of (2)-(4) with $D_{min} = 10^{-4}$ and with S_0 in the range $3\times10^{-4} \leftrightarrow 10^{-2}$. For this D_{min} the loading-unloading cycle is quasi-periodic, leading to a clearer identification of the signatures of loading and unloading vs. other phenomena in the statistical results that we present below.

Loading-unloading cycle. The total field energy at any instant can be defined as

$$E(t) = \int dz\, B_x^2(z,t) \tag{10}$$

Figure 2 shows the evolution of this quantity for four integrations of the system (2)-(4) with D_{min} fixed and over a large range in source strengths. These four runs will be referred to as R1 – R4 for the remainder of this paper. The results shown follow early transients from arbitrary initial states that are not included in the figure.

It is possible to set the source strength $S(z)$ to a low enough value so that field annihilation at the rate set by $D(z,t) = D_{min}$ is sufficient to balance the rate of field reversal growth induced by the source. In this case the system settles into a simple steady diffusion state. The distribution of field in this case is qualitatively similar to the average state in Figure 1. The slope of the distribution self adjusts so that the field annihilation rate equals the reversal

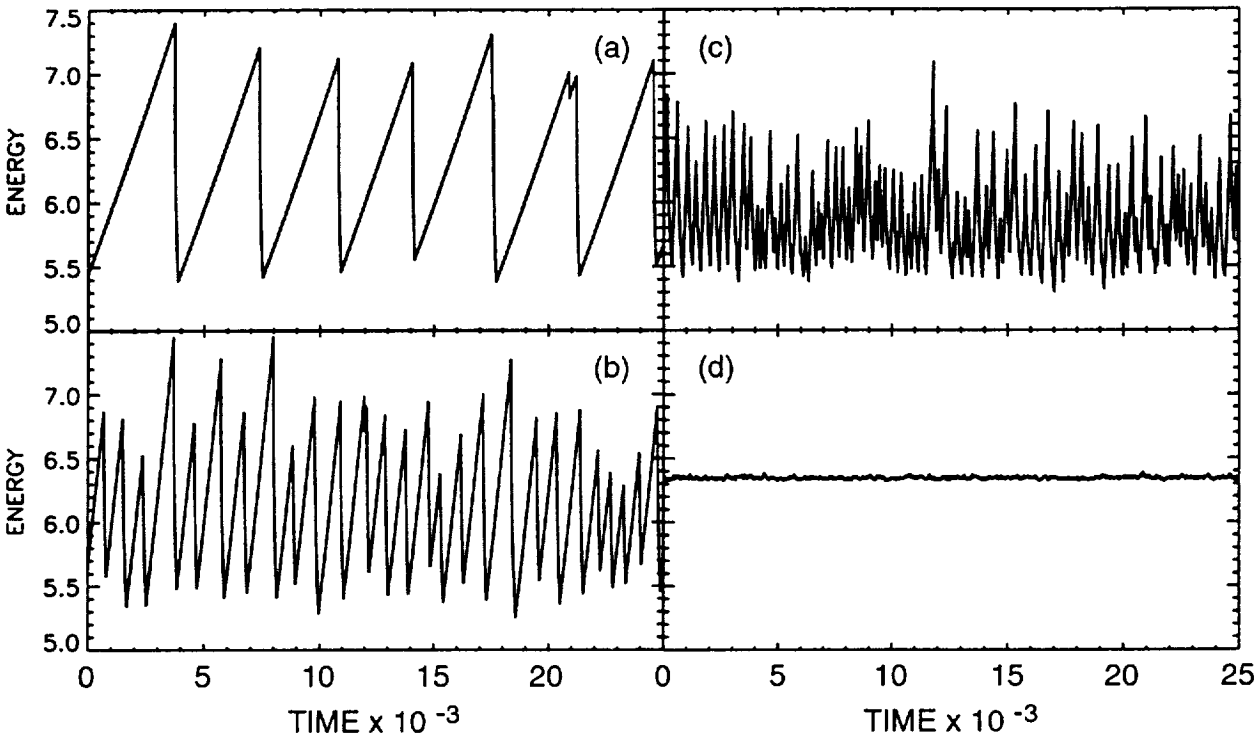

Figure 2. Evolution of the total field energy with $D_{min} = 10^{-4}$ and $S_0 = 3\times10^{-4}$ (a), $S_0 = 10^{-3}$ (b), $S_0 = 3\times10^{-3}$ (c), and $S_0 = 10^{-2}$. The average total energy does not vary significantly over a large range of source strengths.

growth rate. If the source strength is increased, however, the slope of the distribution must increase accordingly. At some source strength a steady state distribution becomes impossible since it requires a slope somewhere on the distribution that is equal to the critical slope. There is a transition at that critical source strength into the time-dependent loading-unloading type of evolution shown in Figure 2a-c. In panel (a), the source strength is just above the transition source strength. In that case, the loading-unloading cycle has its largest amplitude and, though irregular, longest period. At the larger source strength of panel (c), the loading-unloading cycle is decreased slightly in amplitude and increased considerably in frequency. In panel (d) the system has made a transition into an entirely different type of behavior; this behavior will be discussed further below.

An important point to notice in Figure 2 is that the average total energy, and therefore the average global distribution of field, is essentially unchanged over the entire range of source strengths (including larger source strengths that are not shown). Because of the presence of a criticality in the dynamics of the system (2)-(4), a ceiling is imposed on the slope of the field distribution, and therefore on the strength of the field reversal. The source continuously drives the distribution toward that ceiling, but on reaching it the field annihilates sufficiently to move its distribution away from the ceiling slope. The field distribution is exceedingly dynamic and far from equilibrium ($B_x(z,t)=0$) at all times. Nevertheless, the result is a stable average global configuration and a well-defined loading-unloading cycle. This stability is a direct consequence of the criticality in the system; it has nothing to do with the possibility of a ground or equilibrium state in the system.

The rate at which magnetic field is driven into the field reversal region by the source function $S(z)$ increases from R1 to R4 by a factor of 30. But the average total field energy in the field reversal region is approximately unchanged from R1 through R4. Thus, we can conclude that the rate at which magnetic field is annihilated also increases by a factor of 30 from R1 to R4. The dynamic behavior illustrated below in Figure 3 and Plate 1 allows for magnetic field annihilation at a rate that is controlled by the rate at which magnetic field is driven into the field reversal region; this driven annihilation rate can be considerably larger than the basic steady diffusion rate. The fundamental process that is involved is diffusion, but it is a dynamic diffusion process that we will call "fast diffusion."

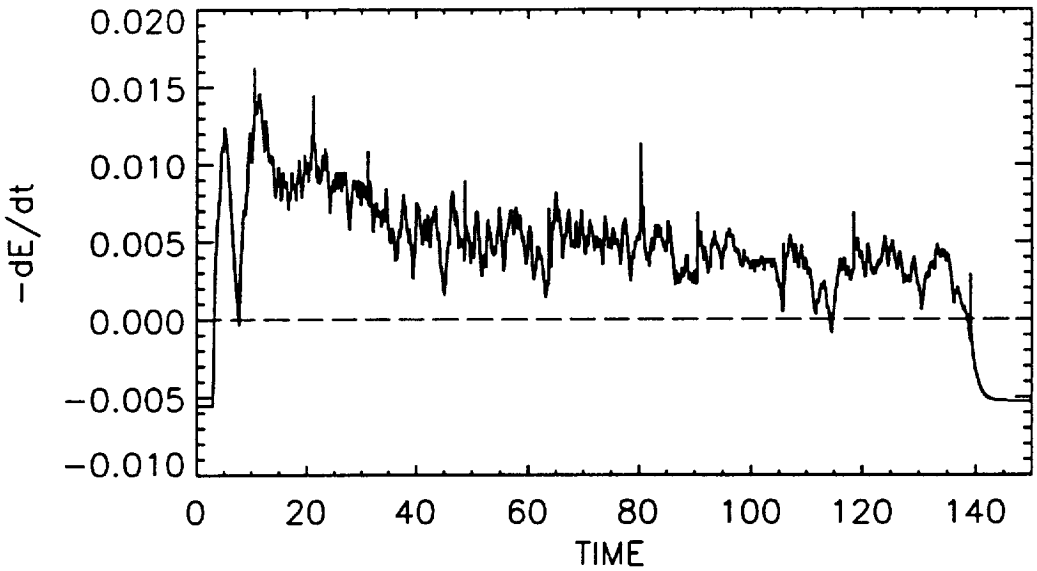

Figure 3. Negative derivative with respect to time of the total energy taken from a single unloading in panel (c) of Figure 2.

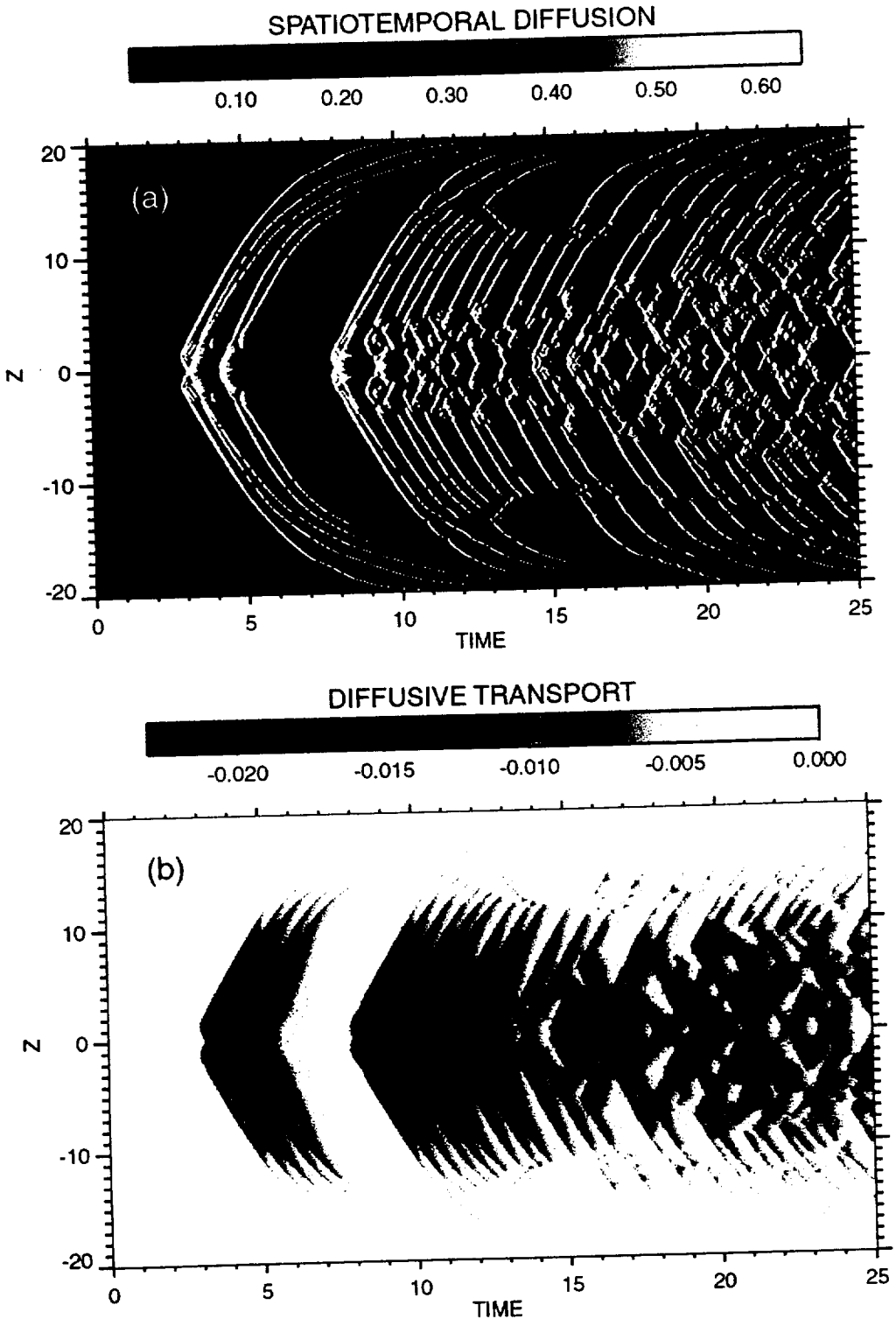

Plate 1. Details of an initial portion of the unloading event shown in Figure 3. (a) Evolution of the diffusion coefficient $D(z,t)$. White dots show grid points at which the current driven instability is excited. (b) Diffusive field transport in response to the growth of $D(z,t)$.

Unloading event. Figure 3 gives another representation of one of the unloading events shown in Figure 2c (R3); the total energy is differentiated with respect to time and plotted with inverted sign. Initially, $-dE/dt$ is negative and steady; the source $S(z)$ steadily loads energy into the system and there is no internal evolution of consequence. The unloading that follows is intense initially, but decays gradually until the system abruptly returns to a quiet state in which loading begins again.

Unloading is the result of many self-organized current sheets ($Q(z,t) = D_{max}$) propagating as waves over the field distribution and leading to field annihilation. The field distribution, during this unloading, appears highly variable over many spatiotemporal scales. An example is given in Plate 1 that corresponds to the initial portion of the unloading event shown in Figure 3 (note the time variable on the abscissae of the two figures). Panel (a) of Plate 1

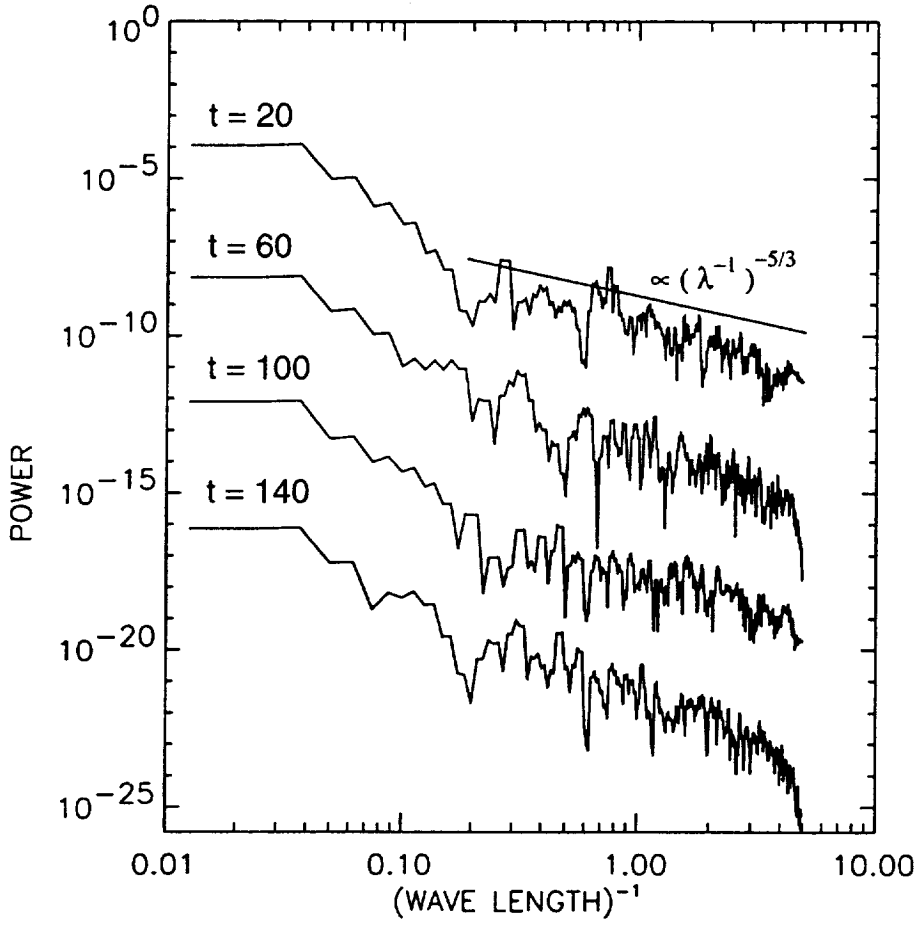

Figure 4. Spatial power spectra as functions of inverse wavelength at four times during the unloading event shown in Figure 3. Spectra have been displaced downward by two decades each for clarity. For reference, a power law curve with spectral index –5/3 has been inserted.

shows the evolution of the diffusion coefficient $D(z,t)$. The white dots on that panel indicate grid points at which the current driven instability is excited; i.e., grid points at which $Q = D_{max}$ according to the criteria in (4). These are grid points at which the current is intense relative to neighboring grid points. It can be seen that these are thin current sheets that maintain themselves and propagate as waves, initially predominantly toward the spatial boundaries but later with no preferred direction except near the boundaries. The initial behavior of the current sheets is more organized while later they appear more disorganized and sporadic. It can be seen that $D(z,t)$ grows rapidly at the positions of the current sheets and then later decays (with time-scale τ). Panel (b) of Plate 1 shows the diffusive field transport $-D\partial B_x/\partial z$ that originates in response to the growth of $D(z,t)$. This transport carries positive field into the region of negative field, ultimately leading to the annihilation of both. Note that, as expected, there is no transport at the spatial boundaries due to the gradient free boundary conditions that have been imposed.

Spatial field structure. To investigate the spatial structure of the field distribution during the unloading event shown in Figure 3 and Plate 1, we have Fourier transformed the spatial distribution at four times during the event; early in the unloading, twice in the middle of the event, and at its end. The sawtooth waveform underlying the non-periodic field distribution has been removed in each case. Figure 4 shows the spatial power spectra at these times plotted versus inverse wavelength from the longest wavelength allowed down to the Nyquist wavelength on the integration grid. The excess power at long wavelengths is due to the response of the system to the sinusoidal source

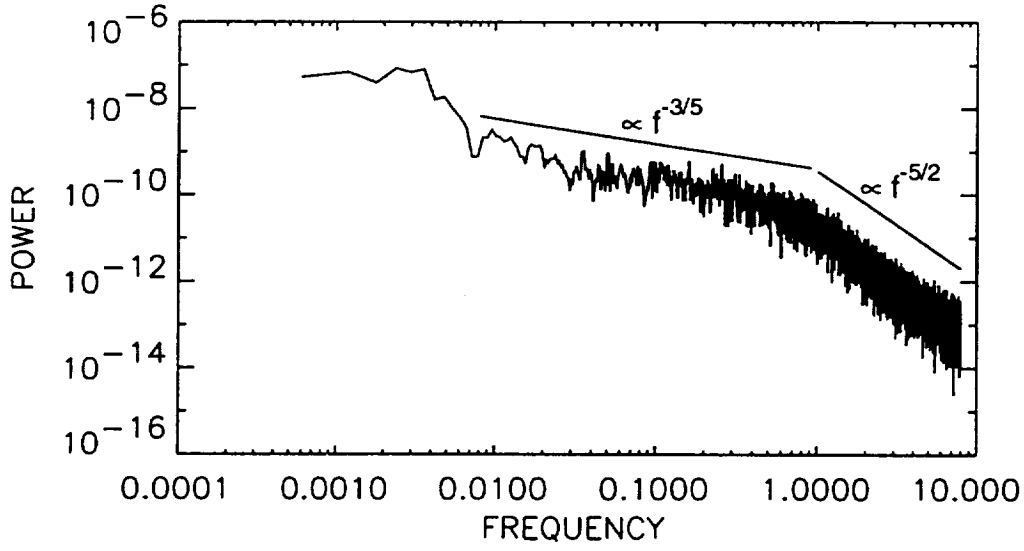

Figure 5. Temporal power spectrum for the field $B_x(z,t)$ at a fixed position. From a portion of the integration R3. Power-law spectra have been added for reference.

$S(z,t) = S(z) = S_0 \sin(\pi z / 2L)$. It can be seen that the spectra are power-laws in inverse wavelength for shorter wavelengths, at all four times, with the exception, sometimes, of the very shortest wavelengths. These spectra indicate self-similar spatial structure in the field over somewhat more than a decade in spatial scales down to those approaching the grid spacing; as the grid spacing is approached the field becomes relatively smooth.

Temporal field structure. Figure 5 shows a power spectrum constructed from a time series formed by sampling $B_x(z,t)$ at a fixed position z in the output from R3. A fixed position close to $z = 0$ has been chosen to produce this result. The peak at the lowest frequencies shows the contribution of the loading-unloading cycle to the variability in the time series; it is indicative of the distribution of time intervals between unloading events. Farther from $z = 0$ the loading-unloading peak is larger but the remainder of the spectrum is essentially unchanged; this remainder is representative of the spectra found at other positions and for other intervals in the integration output. There are clearly two scaling regions in the spectrum. A comparison with Figure 3 shows that the portion of the spectrum that is reasonably approximated by a power-law with spectral index –3/5 contains time scales that range from the typical duration of an unloading event down to the growth and decay time-scale of the diffusion coefficient $\tau = 1$. This portion of the spectrum is due to the wave-like phenomena on the field distribution during the unloading intervals. Beyond the kink at $f \approx 1$ there is a second power-law spectral region with a steeper spectral index. The time scales involved in this portion of the spectrum are well resolved by both the integration time step and the output-sampling interval. We show below that this portion of the spectrum is due to the formation and decay of isolated current sheets that do not last long enough to propagate and interact with other current sheets.

Discussion of spatiotemporal field structure. From these results, it can be seen that the presence of internal field "turbulence" is consistent with the execution of the loading-unloading cycle. It is important to realize, in addition, that the presence of the internal turbulence is also necessary to generate the loading-unloading cycle. From the first three panels of Figure 2, it can be seen that at any one value of total energy the system can be in one of two possible states, loading or unloading. The difference between these two states is the absence or presence of internal turbulence. One can imagine a field distribution like the average one shown in Figure 1, but also containing weak spatial perturbations, too weak to bring the distribution into criticality at any position. As the source drives the distribution slope (current sheet strength) upward, however, the critical gradient eventually must be reached at some point on the distribution. Figure 6 is a sketch of the field evolution that we have observed near the point of criticality just after the critical gradient is exceeded. Unstable current-sheet waves propagate away from the point of criticality. Flux is transported rapidly by these current sheets with the consequence that even steeper gradients are generated in their vicinities; the current sheets become self-sustaining. As time increases, the field distribution becomes exceedingly dynamic; more waves are excited and more regions containing steep gradients are generated. The result is a

self-sustaining avalanche of flux through the system. Even as the system loses energy, it still remains at criticality at various propagating spatial positions because the localized current sheets generate steep gradients in their vicinities that far exceed the critical gradient. It is this property of the turbulence that keeps the system in contact with criticality even when the total system energy has decreased considerably below that necessary to bring the system into criticality initially. Eventually the wave activity may stop, however, and in the absence of wave activity a considerable amount of energy must then be added to the system to bring it back to criticality again. In this way, a loading-unloading cycle is created. It can be seen that the turbulence is more than compatible with the loading-unloading cycle, it is actually necessary in order to produce the loading-unloading cycle.

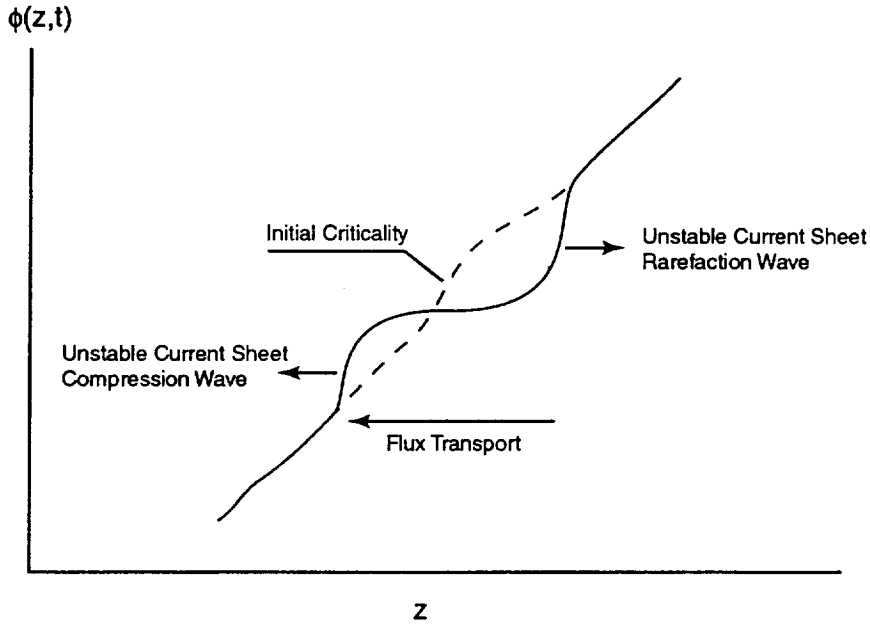

Figure 6. Sketch of initial field evolution following criticality at a point on the field distribution.

A further study of this turbulence phenomenon has shown that it is ultimately the hysteresis in Q, as defined by (4), that leads to the loading-unloading cycle. In order for the current sheets to generate nearby steep gradients, the local flux transport must be fast; effectively, large values of the diffusion coefficient must develop locally. Since the diffusion coefficient grows exponentially with time-scale τ, the local instability must persist long enough, on this time-scale, to allow the diffusion coefficient growth. The persistence of the local instability is the result of the hysteresis in Q. On setting $\beta = 1$ in (4), we have found that the loading-unloading cycle vanishes; organized self-sustaining current sheets do not form.

Burst size and duration distributions. The (negative) derivative with respect to time of the total field energy is shown in Figure 3 for a single unloading event. From Figure 3, it can be seen that a burst size

$$\Delta E = \int_{\Omega} \left[\left(-\frac{dE}{dt}(t) \right) - L_E \right] dt \tag{11}$$

can be defined in which Ω is the time interval that begins when $-dE/dt$ crosses the level L_E in the positive direction and ends when $-dE/dt$ crosses the level L_E in the negative direction. If $L_E = 0$, then the burst size ΔE is the energy lost from the field during the duration interval Ω; more generally, it is the area bounded above by the curve $-dE/dt$ and below by the level L_E. It can be seen from Figure 3 that the result would depend critically on the choice of L_E. By setting $L_E = -.004$ a single large burst would be found. With $L_E = 0$ perhaps three or four somewhat smaller bursts would be defined. And, with $L_E = .003$ one or two bursts from the beginning of the unloading event would be discovered, and many smaller bursts would be found due to the internal evolution of the unloading event during its relaxation. In this case, both internal and global unloading bursts would be defined.

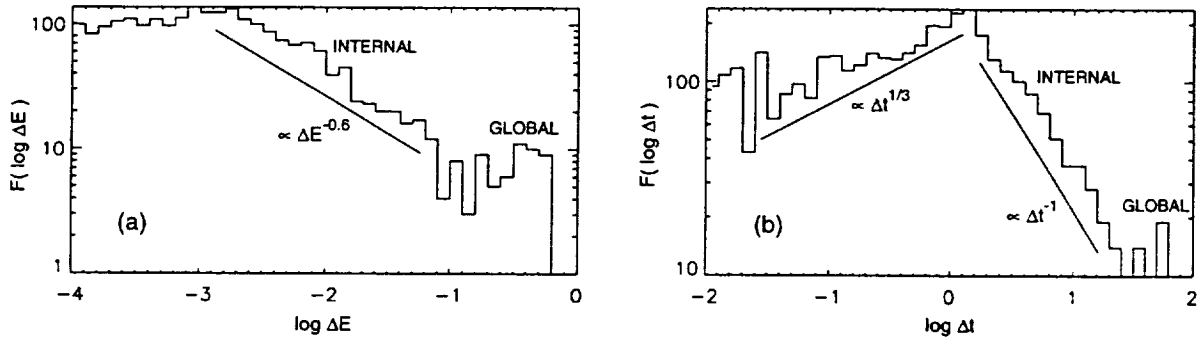

Figure 7. Burst size (a) and duration (b) distributions computed from the derivative with respect to time of the total energy shown in panel (c) of Figure 2. $L_E = .003$.

Power law distributions of burst size and duration in sandpile models and in physical systems are considered indicators of self-organized criticality [*Bak et al.*, 1987; 1988; *Lu*, 1995a; *Consolini*, 1997]. Using $L_E = .003$, burst size and duration (Ω) distributions have been constructed as explained in the previous paragraph for the total field energy in R3, shown in panel (c) of Figure 2. Panel (a) of Figure 7 shows the distribution in $\log \Delta E$ of burst size and panel (b) shows the distribution in $\log \Delta t$ of burst duration. By varying L_E, as explained above, we have determined that the peaks in these distributions that are labeled "global" are measures of the global unloading event statistics and the remainder of the distributions are measures of the internal evolution of the unloading events. It can be

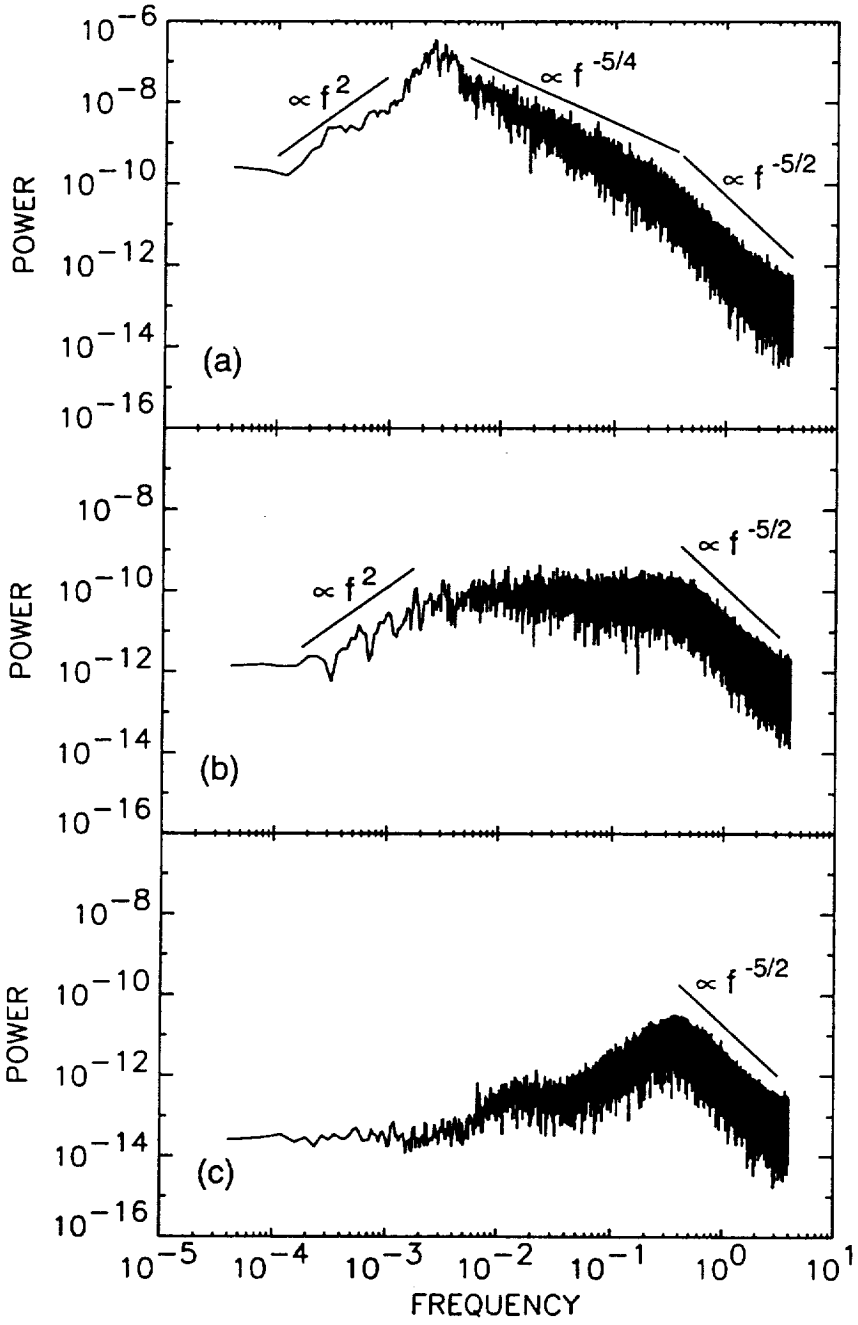

Figure 8. Power spectra constructed from the time series dE/dt obtained from the outputs of integration (a) R3 (Figure 2, panel (c)), (b) R4 (Figure 2, panel (d)) and (c) R4 with $\beta = 1$. Several scaling regions are indicated.

seen that the global unloading events have well defined amplitude and time scales associated with them, but the internal events are broadly distributed in size and duration. Both distributions show power law shapes with a spectral break. As in the case of the power spectrum shown in Figure 5, the duration distribution exhibits its spectral break at the time-scale $\tau = 1$, the time-scale over which the diffusion coefficient evolves. The burst size distribution, in par-

ticular, is reminiscent of that obtained by *Chapman et al.* [1998] in their study of a sandpile model. We conclude, as they did, that these distributions indicate internal SOC dynamics plus global unloading events with well-defined size and time scales. The results shown in Figure 7 show, in addition, a spectral break at the basic time-scale $\tau = 1$ of the system (2)-(4).

Power spectra. Hwa and Kardar [1992] have studied power spectra constructed from the energy dissipation rate time series of a 1-dimensional running sandpile model. As they increased the rate at which they loaded the sandpile, three scaling regimes emerged in the spectra. They found: (1) A high frequency regime dominated by isolated avalanches on the sandpile; (2) an intermediate frequency regime, called the hydrodynamic regime, in which avalanches interact with each other; and (3) a low frequency regime dominated by anticorrelated system-wide discharges. We have constructed power spectra from the analogous time series dE/dt and have found similar results, although our interpretation of the results is somewhat different, due primarily to the different nature of the system (2)-(4) as compared to their sandpile model. The power spectra are shown in Figure 8; they have been constructed from the time derivative of the total energy in the output of R3 (8a) and R4 (8b), plus (8c) the output of an additional integration in which all parameters were identical to those in R4 except for $\beta = 1$.

The sole difference between the integrations R3 and R4 is that the strength of the source $S(z)$ was increased by a factor of 3, resulting in the loss of the loading-unloading cycle in R4 as discussed above. The effects of this loss are shown dramatically in Figure 8. As mentioned above, the series of integrations discussed in this paper was chosen for its somewhat high value of D_{min}, with the consequence that the loading-unloading cycle is quasi-periodic. In panel (a) of Figure 8, the peak at $f \approx 3\times10^{-3}$ is at the frequency of recurrence of the unloading events. The scaling regime with spectral index –5/4 covers the range of time-scales from the typical duration of the unloading events down, almost, to the fundamental time-scale of the system $\tau = 1$. It is over this range of time-scales that the system exhibits wave-like behavior (Plate 1) with the propagation of self-organized, self-sustaining current sheets throughout. If these are the analogues of avalanches in a sandpile model, then these "avalanches" are clearly interacting with each other in this time-scale range; this is the hydrodynamic regime in this continuum model. In R4, the loading-unloading cycle was quenched. Consequently, in panel (b) the loading-unloading peak is gone and the hydrodynamic scaling regime exhibits itself as white noise; there appears to be no dependence on frequency at all in this regime.

The power spectra in panels (a) and (b) of Figure 8 exhibit similar high frequency scaling regimes (spectral index $\approx -5/2$); the spectral indices and the amplitudes are approximately equal. For their sandpile model, *Hwa and*

Kardar [1992] interpreted this regime as due to the contribution of isolated non-interacting avalanches to the evolution of the pile. A close examination of Plate 1, panel (a), shows that there are instances of brief, isolated current sheets, particularly in the range $t = 20 - 25$. To investigate the possibility that these brief, isolated current sheets are contributing this scaling regime to the power spectrum, we have repeated R4 with the parameter $\beta = 1$. With $\beta = 1$ self-sustaining current sheets do not form. All instances of current sheet formation are very brief; they form sporadically and they do not propagate nor do they interact. Of course, there also is no loading-unloading cycle. Panel (c) of Figure 8 shows the power spectrum obtained in this case. The high frequency scaling regime remains but the rest of the spectrum is diminished considerably compared to that shown in panel (b). From this result, we conclude that the high frequency scaling regime is a consequence of isolated non-interacting current sheets, analogous to the non-interacting avalanches in the study of Hwa and Kardar.

In addition, Hwa and Kardar found a low frequency scaling regime in their power spectra produced by anticorrelated system-wide discharges. Panels (a) and (b) of Figure 8 show the possibility of a low frequency scaling range with spectra rising rapidly with frequency. However, the analogy between the Hwa and Kardar sandpile and the Lu model, system (2)-(4), appears to fail at this point. We have found no system-wide discharges (all grid points unstable simultaneously) in the evolution of the solutions of (2)-(4) which we have studied. The largest events in the solutions are the unloading events, and they are composed of wave-like behavior in the hydrodynamic regime.

Steady fast diffusion. At the high source strength used in R4, the field reversal solutions of the Lu model exhibit an entirely different type of behavior in which there is no loading-unloading cycle; this behavior is shown in panel (d) of Figure 2. We have examined the output of R4 in the format used in Plate 1 and have found that it looks very much like the last portion of Plate 1, in the interval $t = 20 - 25$. Panel (a) of Figure 9 gives an indication of how this behavior develops. To obtain Figure 9a, we have continued R4, but with $S(z) = 0$, long enough for the system to come to a quiet state; this is the case at $t = 0$ in Figure 9a. As indicated in the figure, the source was later turned back on to the R4 level. The system immediately went into a loading phase until a significant unloading developed. Comparing Figures 9a and 3, it can be seen that following the unloading the system could not recover as it did in the lower driver strength R3. The source is strong enough to keep the system in contact with criticality continuously; the system is pinned against the criticality ceiling. It responds by unloading continuously at a low level in the disorganized fashion shown in the latter portion of Plate 1. As we have noted above, we call this behavior "fast diffusion" to indicate that it is a diffusive process, but a very dynamic one whose rate is high and controlled by the strength of the source. In this case, the strength of the source is fixed by the rate at which field is convected into the field reversal region.

Figure 9b shows the effect of turning the source off in the middle of a steady fast diffusion event. Because unloading is already in progress at the rate necessary to balance the source strength, when the source is turned off the system responds immediately with an unloading event that is indistinguishable from such an event in a loading-unloading cycle. Of course, in this case, the system can eventually recover to a quiet state because the source has been turned off.

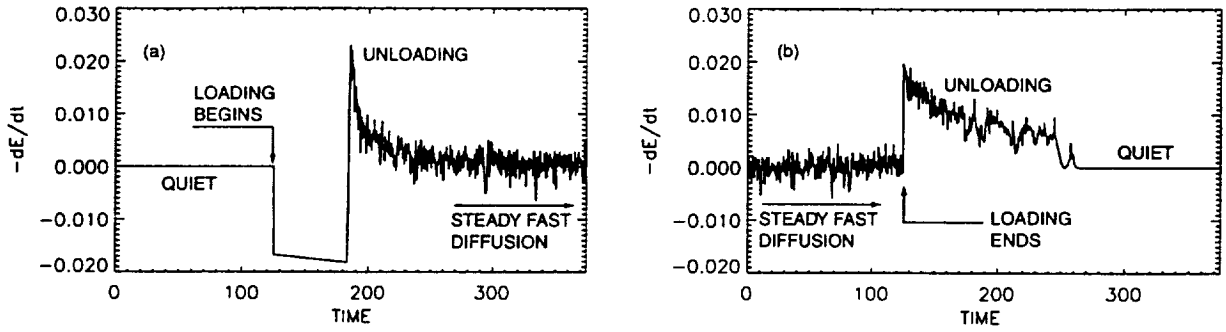

Figure 9. Time derivative of the total energy showing the (a) beginning and (b) end of a steady fast diffusion interval similar to that shown in panel (d) of Figure 2 for R4. To obtain these results, all model parameters were set to those used to obtain R4 except that the source $S(z,t)$, initially off, was turned on and then off again.

During extended intervals ($\geq 4-6$ hrs.), when the interplanetary field is turned strongly southward and the solar wind parameter VB_s is strong and steady, the magnetosphere responds with a behavior that has been called steady magnetospheric convection (SMC) [*Sergeev et al.*, 1996a]. These events have been observed to begin and end with a substorm, but during an event the global magnetosphere is stable; there is no evidence of global substorm activity. Nevertheless, during these events high latitude ground magnetometers detect considerable short-term (< 10 min) impulsive transients that could be interpreted, under other circumstances, to be due to substorm activity, and the magnetotail plasma sheet contains significant transient activity on short (~ 1 min) time scales. At = 20 R_E characteristic features include earthward flow bursts, energetic particle bursts, and dipolarizations associated with the flow bursts [*Sergeev et al.*, 1996a]. The plasma sheet is quite active in a manner that is reminiscent of the BBF and fast flow phenomena discussed by *Baumjohann et al.* [1990], *Angelopoulos et al.* [1992; 1994; 1996], and *Fairfield et al.* [1998; 1999]. Steady magnetospheric convection, as the name implies, has been explained in terms of convection in the plasma sheet [*Hau et al.*, 1989], but, to our knowledge, the deep minimum in the tail magnetic field required by this explanation has not been found.

The field reversal solutions of the Lu model that are discussed in this paper are far too idealized to draw definitive conclusions concerning reconnection in the magnetotail. However, the steady fast diffusion behavior does suggest

an alternate explanation for the SMC events. In analogy to steady fast diffusion, we suggest that a SMC event is an extended recovery phase in the magnetotail that cannot go to completion because the VB_z driver is too strong. The magnetotail may be driven into criticality continuously, resulting in a state of steady low level unloading that balances the strong, steady input. Observations in the magnetotail should reveal multiple, isolated, sporadic reconnection sites distributed in the plasma sheet; fast flows and BBFs should be associated with these sites. In this manner, both the global stability and the simultaneous mesoscale activity discussed by *Sergeev et al.* [1996a] can be incorporated into the explanation for SMC events, and SMC events can be merged naturally within the NENL substorm model.

V. Summary

We have reviewed a considerable body of evidence that indicates there is a SOC component in the dynamics of the plasma sheet that contributes to the characteristics of the substorm phenomenon. In analogy to the behavior of sandpile models when they are in SOC, we view observations of BBFs, fast flows, localized dipolarizations, etc. as evidence that multiple localized reconnection sites provide the basic avalanche phenomenon in the establishment of SOC in the plasma sheet.

In this paper, we have presented the results of our first step toward a plasma physical model of the SOC component in the plasma sheet. We have studied a resistive MHD model of a magnetic field reversal. The anomalous resistivity is self consistently generated in this model in response to the excitation of an idealized current driven instability. We have shown that, when driven by convection of magnetic flux into the field reversal region, the model is able to produce rapid magnetic field annihilation through a dynamic behavior that has many of the characteristics of a system in SOC.

Although our model is a highly idealized model of the field reversal in the plasma sheet, we feel that there are already several implications that can be drawn from its behavior that may help in understanding the substorm phenomenon, while indicating directions for further study:

We find that the global state of the field reversal is remarkably stable, essentially invariant under a wide range of source strengths and, consequently, field annihilation rates. This stability is due to the existence of a criticality ceiling in the dynamics of the field reversal. The system self-adjusts to this ceiling from below and, while very dynamic internally, always resides near this ceiling, far from its ground, or equilibrium, state. This residence in the vicinity of criticality is a characteristic property of systems that are driven into SOC. In the case of our model of a field reversal, the annihilation rate self-adjusts to the rate at which magnetic flux is introduced into the field reversal region so

that the global state of the field remains everywhere near criticality. We suppose that this self-adjustment is also a property of the magnetotail dynamics. In its ground state, the magnetosphere would contain a dipole magnetic field stretching to great distances from Earth. Under the influence of the solar wind, the magnetosphere resides far from its ground state, with a magnetotail in a self-organized state that is always near criticality, as evidenced by the observation of BBFs, fast flows, plasma sheet turbulence, etc. at all substorm phases. The rate at which magnetic flux is processed through the magnetotail depends on the rate at which it is introduced. The magnetotail self-adjusts to maintain this balance, thereby maintaining a stable global configuration. This stability is a consequence of the criticality in the magnetotail field reversal, and is unrelated to the existence of a ground state in the system.

A principal goal in our research is to understand the compatibility of the coherent, predictable substorm cycle with strong turbulence in the key plasma sheet component of the substorm dynamics. How can the slow approach to a critical state in the thinning plasma sheet be understood in light of the very dynamic nature of the plasma sheet that is observed? We have found that, under the influence of a steady driver, our field reversal model can enter a predictable quasi-periodic loading-unloading cycle that is not only compatible with the existence of "turbulence" in the field reversal, it is a consequence of the turbulence. Following contact with criticality at a position in the field reversal, strong, propagating, self-sustaining current sheets are formed. These current sheets perturb the nearby field in such a way as to induce criticality nearby, thereby producing more current sheets with the same property. An avalanche is formed, with the property that the field retains contact with criticality after the field energy in the system has fallen well below that which was necessary to bring the system into criticality originally. Later, when the system eventually does quiet down, a significant amount of energy must be added to bring it back to criticality again. In this way, a loading-unloading cycle is formed. We have found that it is the hysteresis, suggested by *Lu* [1995a], in the current driven instability that is, at root, the source of this behavior. From these results, we would suggest that in the plasma sheet, whatever the cause of criticality, the response of the plasma sheet (we feel, through localized reconnection) must force nearby positions into criticality, the result being a self-sustaining avalanche that is able to persist even as the field energy drops below that necessary to produce the onset of the avalanche. If the solar wind driver remains steady, a loading-unloading cycle may result. Understanding the cessation of this process would provide an understanding of the substorm recovery phase [*Baker et al.*, 1999]. We will search for this behavior as we generalize our field reversal model toward a more realistic plasma sheet model.

We have found that when we drive the field reversal model steadily and strongly enough the loading-unloading cycle vanishes. The global state of the field reversal is pushed so close to criticality, the perturbations on the field distribution cannot lose contact with criticality. Recovery from unloading never ends and the system goes into a quasi-steady annihilation state containing current sheets everywhere propagating in a disorganized fashion. The an-

nihilation rate is high when compared to the average rate in the case of loading and unloading, but low compared to the peaks in the unloading intervals. Still, a balance between magnetic flux input and field annihilation is achieved. The global state of the field distribution is very steady but, internally, it is quite dynamic. This behavior is analogous to that seen in the magnetosphere during intervals called steady magnetospheric convection events. During these events the solar wind is unusually steady with the interplanetary magnetic field turned southward, there is no evidence for global substorm activity, but there is considerable activity on smaller scales in the plasma sheet with responses in the ionosphere and on the ground that otherwise look like substorm activity [*Sergeev et al.*, 1996a]. We suggest that this behavior is the result of steady, low-level unloading as a consequence of a substorm recovery that could not complete. It is likely that this condition results when the plasma sheet has been driven too close to criticality over an extended spatial domain as a consequence of an unusually strong and steady magnetic flux input to the tail. We would expect to find localized reconnection sites distributed over the spatial domain of near criticality. We believe the name, steady magnetospheric convection, is a misnomer, the plasma sheet transport being more closely related to that of BBF and fast flow events.

In the future, we will generalize this model to higher dimensions and couple it to more of the MHD system. In addition, we will consider other kinetic phenomena and attempt to model them as we have the idealized current driven instability in our present work. At each step in our generalization, we will study the evolution of the model into SOC and we will re-examine the conjectures given in the preceding paragraphs. Our goal remains, to give a quantitative characterization of SOC in the plasma sheet and to elucidate its role in the substorm cycle.

Acknowledgments. We are grateful for the support we have received from NASA SR&T grant 344-14-00-02, which has made this research possible.

References

Angelopoulos, V., W. Baumjohann, C.F. Kennel, F.V. Coroniti, M.G. Kivelson, R. Pellat, R.J. Walker, H. Luhr, and G. Paschmann, Bursty Bulk Flows in the Inner Central Plasma Sheet, *J. Geophys. Res.*, *97* (A4), 4027-4039, 1992.

Angelopoulos, V., F.V. Coroniti, C.F. Kennel, M.G. Kivelson, R.J. Walker, C.T. Russell, R.L. McPherron, E. Sanchez, C.I. Meng, W. Baumjohann, G.D. Reeves, R.D. Belian, N. Sato, E. FriisChristensen, P.R. Sutcliffe, K. Yumoto, and T. Harris, Multipoint analysis of a bursty bulk flow event on April 11, 1985, *J. Geophys. Res.*, *101* (A3), 4967-4989, 1996.

Angelopoulos, V., C.F. Kennel, F.V. Coroniti, R. Pellat, M.G. Kivelson, R.J. Walker, C.T. Russell, W. Baumjohann, W.C. Feldman, and J.T. Gosling, Statistical Characteristics of Bursty Bulk Flow Events, *J. Geophys. Res.*, *99* (A11), 21257-21280, 1994.

Bak, P., C. Tang, and K. Wiesenfeld, Self-Organized Criticality - an Explanation of 1/F Noise, *Phys. Rev. Lett.*, *59* (4), 381-384, 1987.

Bak, P., C. Tang, and K. Wiesenfeld, Self-Organized Criticality, *Phys. Rev. A*, *38* (1), 364-374, 1988.

Baker, D.N., L.F. Bargatze, and R.D. Zwickl, Magnetospheric Response to the Imf - Substorms, *Journal of Geomagnetism and Geoelectricity*, *38* (11), 1047-1073, 1986.

Baker, D.N., T.I. Pulkkinen, V. Angelopoulos, W. Baumjohann, and R.L. McPherron, Neutral line model of substorms: Past results and present view, *J. Geophys. Res.*, *101* (A6), 12975-13010, 1996.

Baker, D.N., T.I. Pulkkinen, J. Büchner, and A.J. Klimas, Substorms: A global magnetospheric instability, *J. Geophys. Res.*, *104* (A7), 14601, 1999.

Baker, D.N., T.I. Pulkkinen, M. Hesse, and R.L. McPherron, A quantitative assessment of energy storage and release in the Earth's magnetotail, *J. Geophys. Res.*, *102* (A4), 7159-7168, 1997.

Baumjohann, W., G. Paschmann, and H. Luhr, Characteristics of High-Speed Ion Flows in the Plasma Sheet, *J. Geophys. Res.*, *95* (A4), 3801-3809, 1990.

Borovsky, J.E., R.C. Elphic, H.O. Funsten, and M.F. Thomsen, The Earth's plasma sheet as a laboratory for flow turbulence in high-beta MHD, *J. Plasma Phys.*, *57*, 1-34, 1997.

Carreras, B.A., D. Newman, V.E. Lynch, and P.H. Diamond, A model realization of self-organized criticality for plasma confinement, *Phys. Plasmas*, *3* (8), 2903-2911, 1996.

Carreras, B.A., B.P. van Milligen, M.A. Pedrosa, R. Balbin, C. Hidalgo, D.E. Newman, E. Sanchez, M. Frances, I. Garcia-Cortes, J. Bleuel, M. Endler, C. Ricardi, S. Davies, G.F. Matthews, E. Martines, V. Antoni, A. Latten, and T. Klinger, Self-similarity of the plasma edge fluctuations, *Phys. Plasmas*, *5* (10), 3632-3643, 1998.

Chang, T., Low-Dimensional Behavior and Symmetry-Breaking of Stochastic- Systems Near Criticality - Can These Effects Be Observed in Space and in the Laboratory, *Ieee Transactions On Plasma Science*, *20* (6), 691-694, 1992a.

Chang, T., Path-Integrals, Differential Renormalization-Group, and Stochastic-Systems Near Criticality, *International Journal of Engineering Science*, *30* (10), 1401-1405, 1992b.

Chang, T., Multiscale intermittent turbulence in the magnetotail, in *Substorms-4*, edited by S. Kokubun, and Y. Kamide, pp. 431-436, Terra Scientific, Tokyo, 1998.

Chapman, S.C., N.W. Watkins, R.O. Dendy, P. Helander, and G. Rowlands, A simple avalanche model as an analogue for magnetospheric activity, *Geophys. Res. Lett.*, *25* (13), 2397-2400, 1998.

Consolini, G., Sandpile cellular automata and magnetospheric dynamics, in *Cosmic Physics in the Year 2000*, edited by S. Aiello, N. Lucci, G. Sironi, A. Treves, and U. Villante, pp. 123, SIF, Bologna, Italy, 1997.

Diamond, P.H., and T.S. Hahm, On the Dynamics of Turbulent Transport Near Marginal Stability, *Phys. Plasmas, 2* (10), 3640-3649, 1995.

Fairfield, D.H., T. Mukai, M. Brittnacher, G.D. Reeves, S. Kokubun, G.K. Parks, T. Nagai, H. Matsumoto, K. Hashimoto, D.A. Gurnett, and T. Yamamoto, Earthward flow bursts in the inner magnetotail and their relation to auroral brightenings, AKR intensifications, geosynchronous particle injections and magnetic activity, *J. Geophys. Res.*, *104* (A1), 355-370, 1999.

Fairfield, D.H., T. Mukai, A.T.Y. Lui, C.A. Cattell, G.D. Reeves, T. Nagai, G. Rostoker, H.J. Singer, M.L. Kaiser, S. Kokubun, A.J. Lazarus, R.P. Lepping, M. Nakamura, J.T. Steinberg, K. Tsuruda, D.J. Williams, and T. Yamamoto, Geotail observations of substorm onset in the inner magnetotail, *J. Geophys. Res.*, *103* (A1), 103-117, 1998.

Hau, L.N., R.A. Wolf, G.H. Voigt, and C.C. Wu, Steady-State Magnetic-Field Configurations For the Earths Magnetotail, *J. Geophys. Res.*, *94* (A2), 1303-1316, 1989.

Horton, W., and I. Doxas, A low-dimension energy-conserving state space model for substorm dynamics, *J. Geophys. Res.*, *101* (A12), 27223-27237, 1996.

Horton, W., and I. Doxas, A low-dimensional dynamical model for the solar wind driven geotail-ionosphere system, *J. Geophys. Res.*, *103* (A3), 4561-4572, 1998.

Horton, W., M. Pekker, and I. Doxas, Magnetic energy storage and the nightside magnetosphere- ionosphere coupling, *Geophys. Res. Lett.*, *25* (21), 4083-4086, 1998.

Hoshino, M., A. Nishida, T. Yamamoto, and S. Kokubun, Turbulent Magnetic-Field in the Distant Magnetotail - Bottom-Up Process of Plasmoid Formation, *Geophys. Res. Lett.*, *21* (25), 2935-2938, 1994.

Hwa, T., and M. Kardar, Avalanches, Hydrodynamics, and Discharge Events in Models of Sandpiles, *Phys. Rev. A*, *45* (10), 7002-7023, 1992.

Klimas, A.J., D.N. Baker, D.A. Roberts, D.H. Fairfield, and J. Buchner, A Nonlinear Dynamic Analog Model of Geomagnetic-Activity, *J. Geophys. Res.*, *97* (A8), 12253-12266, 1992.

Klimas, A.J., D.N. Baker, D. Vassiliadis, and D.A. Roberts, Substorm Recurrence During Steady and Variable Solar-Wind Driving - Evidence For a Normal-Mode in the Unloading Dynamics of the Magnetosphere, *J. Geophys. Res.*, *99* (A8), 14855-14861, 1994.

Klimas, A.J., D. Vassiliadis, and D.N. Baker, Data-derived analogues of the magnetospheric dynamics, *J. Geophys. Res.*, *102* (A12), 26993-27009, 1997.

Klimas, A.J., D. Vassiliadis, and D.N. Baker, Dst index prediction using data-derived analogues of the magnetospheric dynamics, *J. Geophys. Res.*, *103* (A9), 20435-20447, 1998.

Klimas, A.J., D. Vassiliadis, D.N. Baker, and D.A. Roberts, The organized nonlinear dynamics of the magnetosphere, *J. Geophys. Res.*, *101* (A6), 13089-13113, 1996.

Klimas, A.J., D. Vassiliadis, D.N. Baker, and J.A. Valdivia, Data-derived analogues of the solar wind-magnetosphere interaction, *Phys. Chem. Earth*, *24*, 37-44, 1999.

Lu, E.T., Avalanches in Continuum Driven Dissipative Systems, *Phys. Rev. Lett.*, *74* (13), 2511-2514, 1995a.

Lu, E.T., Constraints On Energy-Storage and Release Models For Astrophysical Transients and Solar-Flares, *Astrophys. J.*, *447* (1), 416-418, 1995b.

Lu, E.T., The Statistical Physics of Solar Active Regions and the Fundamental Nature of Solar-Flares, *Astrophys. J.*, *446* (2), L109-L112, 1995c.

Lu, E.T., and R.J. Hamilton, Avalanches and the Distribution of Solar-Flares, *Astrophys. J.*, *380* (2), L89-L92, 1991.

Lu, E.T., R.J. Hamilton, J.M. McTiernan, and K.R. Bromund, Solar-Flares and Avalanches in Driven Dissipative Systems, *Astrophys. J.*, *412* (2), 841-852, 1993.

Lui, A.T.Y., C.L. Chang, A. Mankofsky, H.K. Wong, and D. Winske, A Cross-Field Current Instability For Substorm Expansions, *J. Geophys. Res.*, *96* (A7), 11389-11401, 1991.

Lui, A.T.Y., C.L. Chang, and P.H. Yoon, Preliminary Nonlocal Analysis of Cross-Field Current Instability For Substorm Expansion Onset, *J. Geophys. Res.*, *100* (A10), 19147-19154, 1995.

Lui, A.T.Y., P.H. Yoon, and C.L. Chang, Quasi-Linear Analysis of Ion Weibel Instability in the Earths Neutral Sheet, *J. Geophys. Res.*, *98* (A1), 153-163, 1993.

Lyons, L.R., T. Nagai, G.T. Blanchard, J.C. Samson, T. Yamamoto, T. Mukai, A. Nishida, and S. Kokubun, Association between Geotail plasma flows and auroral poleward boundary intensifications observed by CANOPUS photometers, *J. Geophys. Res.*, *104* (A3), 4485-4500, 1999.

McPherron, R.L., and T. Hsu, The main onset of the magnetospheric substorm, in *Substorms-4*, edited by S. Kokubun, and Y. Kamide, pp. 79-82, Terra Scientific, Tokyo, 1998.

Milovanov, A.V., L.M. Zelenyi, and G. Zimbardo, Fractal structures and power law spectra in the distant Earth's magnetotail, *J. Geophys. Res.*, *101* (A9), 19903-19910, 1996.

Nagai, T., M. Fujimoto, Y. Saito, S. Machida, T. Terasawa, R. Nakamura, T. Yamamoto, T. Mukai, A. Nishida, and S. Kokubun, Structure and dynamics of magnetic reconnection for substorm onsets with Geotail observations, *J. Geophys. Res.*, *103* (A3), 4419-4440, 1998.

Newman, D.E., B.A. Carreras, P.H. Diamond, and T.S. Hahm, The dynamics of marginality and self-organized criticality as a paradigm turbulent transport, *Phys. Plasmas*, *3* (5), 1858-1866, 1996.

Ohtani, S., T. Higuchi, A.T.Y. Lui, and K. Takahashi, Magnetic Fluctuations Associated With Tail Current Disruption - Fractal Analysis, *J. Geophys. Res.*, *100* (A10), 19135-19145, 1995.

Ohtani, S., K. Takahashi, T. Higuchi, A.T.Y. Lui, H.E. Spence, and J.F. Fennell, AMPTE/CCE-SCATHA simultaneous observations of substorm- associated magnetic fluctuations, *J. Geophys. Res.*, *103* (A3), 4671-4682, 1998.

Papadopoulos, K., Microinstabilities and anomalous transport, in *Collisionless Shocks in the Heliosphere: A Tutorial Review*, edited by R.G. Stone, and B.T. Tsurutani, pp. 59-90, American Geophysical Union, Washington DC, 1985.

Pulkkinen, T.I., D.N. Baker, L.A. Frank, J.B. Sigwarth, H.J. Opgenoorth, R. Greenwald, E. Friis-Christensen, T. Mukai, R. Nakamura, H. Singer, G.D. Reeves, and M. Lester, Two substorm intensifications compared: Onset, expansion, and global consequences, *J. Geophys. Res.*, *103* (A1), 15-27, 1998.

Pulkkinen, T.I., D.N. Baker, D.G. Mitchell, R.L. McPherron, C.Y. Huang, and L.A. Frank, Thin Current Sheets in the Magnetotail During Substorms - Cdaw- 6 Revisited, *J. Geophys. Res.*, *99* (A4), 5793-5803, 1994a.

Pulkkinen, T.I., D.N. Baker, R.J. Pellinen, J. Buchner, H.E.J. Koskinen, R.E. Lopez, R.L. Dyson, and L.A. Frank, Particle Scattering and Current Sheet Stability in the Geomagnetic Tail During the Substorm Growth-Phase, *J. Geophys. Res.*, *97* (A12), 19283-19297, 1992.

Pulkkinen, T.I., D.N. Baker, P.K. Toivanen, R.J. Pellinen, R.H.W. Friedel, and A. Korth, Magnetospheric Field and Current Distributions During the Substorm Recovery Phase, *J. Geophys. Res.*, *99* (A6), 10955-10966, 1994b.

Saito, T., K. Yumoto, and Y. Koyama, Magnetic pulsation Pi2 as a sensitive indicator of magnetospheric substorm, *Planetary and Space Science*, *24*, 1025, 1976.

Sakurai, T., and T. Saito, Magnetic pulsation Pi2 and substorm onset, *Planetary and Space Science*, *24*, 573, 1976.

Sergeev, V.A., R.J. Pellinen, and T.I. Pulkkinen, Steady magnetospheric convection: A review of recent results, *Space Science Reviews*, *75* (3-4), 551-604, 1996a.

Sergeev, V.A., T.I. Pulkkinen, and R.J. Pellinen, Coupled-mode scenario for the magnetospheric dynamics, *J. Geophys. Res.*, *101* (A6), 13047-13065, 1996b.

Takalo, J., J. Timonen, A.J. Klimas, J. Valdivia, and D. Vassiliadis, Nonlinear energy dissipation in a cellular automaton magnetotail field model, *Geophys. Res. Lett.*, *26* (13), 1813, 1999a.

Takalo, J., J. Timonen, A.J. Klimas, J.A. Valdivia, and D. Vassiliadis, A coupled map model for the magnetotail current sheet, *Geophys. Res. Lett.*, in press, 1999b.

Tsurutani, B.T., M. Sugiura, T. Iyemori, B.E. Goldstein, W.D. Gonzalez, S.I. Akasofu, and E.J. Smith, The Nonlinear Response of Ae to the Imf Bs Driver - a Spectral Break At 5 Hours, *Geophys. Res. Lett.*, *17* (3), 279-282, 1990.

Uritsky, V.M., and M.I. Pudovkin, Low frequency 1/f-like fluctuations of the AE-index as a possible manifestation of self-organized criticality in the magnetosphere, *Ann. Geophys.*, *16* (12), 1580-1588, 1998.

Valdivia, J.A., A.S. Sharma, and K. Papadopoulos, Prediction of magnetic storms by nonlinear models, *Geophys. Res. Lett.*, *23* (21), 2899-2902, 1996.

Valdivia, J.A., D. Vassiliadis, A. Klimas, A.S. Sharma, and K. Papadopoulos, Spatiotemporal activity of magnetic storms, *J. Geophys. Res.*, *104* (A6), 12239-12250, 1999a.

Valdivia, J.A., D. Vassiliadis, A.J. Klimas, and A.S. Sharma, Modeling the spatial structure of the high latitude magnetic perturbations and the related current system, *Phys. Plasmas*, in press, 1999b.

Vassiliadis, D., A.J. Klimas, D.N. Baker, and D.A. Roberts, A Description of the Solar-Wind Magnetosphere Coupling Based On Nonlinear Filters, *J. Geophys. Res.*, *100* (A3), 3495-3512, 1995.

Vlahos, L., M. Georgoulis, R. Kluiving, and P. Paschos, The Statistical Flare, *Astron. Astrophys.*, *299* (3), 897-911, 1995.

Yoon, P.H., and A.T.Y. Lui, Nonlocal ion Weibel instability in the geomagnetic tail, *J. Geophys. Res.*, *101* (A3), 4899-4906, 1996.